UNCERTAINTY IN PHOTOCONDUCTANCE LIFETIME MEASUREMENTS THAT USE AN INDUCTIVE-COIL DETECTOR

Keith R. McIntosh[1] and Ronald A. Sinton[2]

[1] Centre for Sustainable Energy Systems, Australian National University, Canberra, ACT 0200, AUSTRALIA

[2] Sinton Consulting, 4720 Walnut St., Suite 102, Boulder, CO 80301 USA

ABSTRACT: Photoconductance (PC) lifetime measurements are used widely within the photovoltaic industry but rarely are the results reported with any uncertainty. While nontrivial to determine, a knowledge of the experimental uncertainty is necessary to distinguish significant from insignificant differences between samples. This paper presents a preliminary study into the experimental uncertainty associated with PC instruments using inductive-coil detectors. Equations that express the uncertainty of (i) the excess carrier concentration and (ii) the effective lifetime are expressed in terms of the uncertainty of the input parameters, such as wafer width, calibration constants, and voltage resolution. The derivations illustrate why there is significantly less uncertainty in parameters extracted through transient rather than quasi-steady-state analyses. The paper also describes the difficulties associated with quantifying PC uncertainties that arise from the implicit relationship between carrier concentration and mobility, from the quantification of calibration errors, and in the case of transient analyses, from the quantification of the error in the voltage decay constant. One transient and one quasi-steady-state example is provided.

Keywords: Calibration, Lifetime, Recombination, Silicon

1 INTRODUCTION

Photoconductance (PC) lifetime measurements are used widely within the photovoltaic industry but rarely are the results reported with any uncertainty. While nontrivial to determine, a knowledge of the experimental uncertainty (or error) is necessary to distinguish significant from insignificant differences between samples.

This paper presents a preliminary study into the experimental uncertainty associated with PC instruments using inductive-coil detectors. It focuses on the WCT-100 [1] applied to crystalline silicon (c-Si), the most widely used lifetime instrument and semiconductor in the photovoltaic industry.

Following a review of the PC procedure, the relevant equations are written in terms of input parameters. This permits a simpler assessment of how the input uncertainties affects the uncertainty of the calculated parameters. It also shows which equations are implicit—an attribute that hinders the formulation of analytic equations to evaluate uncertainty.

The paper comments on the relative importance of the input uncertainties for transient and quasi-steady-state analyses, providing experimental examples of each.

2 GENERAL PC PROCEDURE

Inductive-coil PC lifetime experiments usually follow the procedure now described; in so doing, they invoke the assumptions listed in Appendix A.

A sample is first placed above a calibrated inductive coil and illuminated by a flash lamp. The coil's output voltage $V(t)$ is recorded and converted to the sample's conductance $S(t)$ by some calibration curve. In the case of the WCT-100, a linear calibration is generally sufficient, but shallow parabolas are also used:

$$S = aV^2 + bV + c\ , \qquad (1)$$

where $a = 0$ for a linear calibration. Hence, the excess conductance $\Delta S(t)$ is given by

$$\begin{aligned}\Delta S(t) &= a\left[V(t)^2 - V_0^2\right] + b\left[V(t) - V\right] \\ &= \Delta V(t)\cdot\left\{a\left[V(t)+V_0\right]+b\right\}\end{aligned}, \qquad (2)$$

where V_0 is the equilibrium voltage prior to illumination.

From the excess conductance $\Delta S(t)$, the excess carrier concentration in the quasi-neutral base Δn can be calculated from

$$\Delta n(t) = \frac{\Delta S(t)}{q \cdot W \cdot \mu_s(\Delta n)}\ , \qquad (3)$$

where, q is the elementary charge, W is the thickness of the quasi-neutral base, and μ_s is the sum of the carrier mobilities. This excess carrier concentration Δn is important to lifetime studies because many recombination mechanisms are proportional to its magnitude—or to the square or cube of its magnitude. Its calculation from (3) is more complicated than it first appears due to the dependence of μ_s on Δn, which is constant at low Δn but decreasing at high Δn (see Appendix B).

Simultaneous to the measurement of $V(t)$, the voltage of a reference detector $V_{ref}(t)$ is measured. This detector is calibrated to the photogeneration rate $G(t)$ within the due to the illumination,

$$G(t) = \frac{kV_{ref}(t)}{W}\ , \qquad (4)$$

where k is a calibration constant that converts V_{ref} to a generation current density, and the W is included to convert that current density into a generation rate (in cm^{-3}). Clearly, this relies on the detector having a linear relationship with illumination intensity.

The output voltages are then used to determine the sample's effective lifetime τ_{eff} as a function of Δn, where τ_{eff} is defined from the total recombination rate U by

$$U = \frac{\Delta n}{\tau_{eff}(\Delta n)}\ . \qquad (5)$$

and where U relates to G and $\Delta n(t)$ by the equation

$$\frac{d\Delta n}{dt} = \dot{n} = G - U \ , \tag{6}$$

which simply states that changes in Δn arise from generation and recombination. Thus, combining (5) and (6) gives

$$\tau_{eff}(\Delta n) = \frac{\Delta n(t)}{G(t) - \dot{n}(t)} \ , \tag{7}$$

which is the well known generalised equation for PC experiments [2]. When $G(t)$ is negligible, the "transient analysis" is sufficient [3], and when $\dot{n}(t)$ is negligible, the quasi-steady state (QSS) analysis is sufficient [4].

It is common for PC experiments to involve comparisons of $\tau_{eff}(\Delta n)$ between samples fabricated by different methods. Conclusions are then drawn about the relative—or sometimes absolute—difference in the recombination associated with those fabrication methods. Although critical to the comparison, the associated experimental uncertainty is almost always omitted, probably because its quantification is difficult. This paper presents a preliminary examination of the factors that contribute to the uncertainty in τ_{eff} and Δn; a more thorough examination will be published elsewhere. We limit the study to the case where the assumptions in Appendix A are valid

3 EQUATIONS IN TERMS OF INPUT PARAMETERS

The uncertainty associated with a calculated parameter is best investigated by expressing the parameter in terms of its experimental inputs. For clarity, the expressions for Δn and τ_{eff} are now derived in terms of the input parameters for a linear PC calibration ($a = 0$), which is adequate for the examples in Section 5.

3.1 Excess carrier concentration Δn

Combining (2) and (3) gives

$$\Delta n = \frac{\Delta V b}{q W \mu_s(\Delta n)} \ . \tag{8}$$

The rules of Appendix C can then be employed to find the uncertainty in Δn due to uncertainty in the input parameters: $\delta\Delta V$, δb, δW and $\delta\mu_s$. The procedure permits the derivation of an analytical equation for $\delta\Delta n$ over the range of Δn where $\mu_s(\Delta n)$ is constant, but is otherwise more complicated due to the implicit nature of (8). As illustrated in Section 5, this uncertainty constitutes the x-axis error bars in a plot of $\tau_{eff}(\Delta n)$.

3.2 Effective lifetime τ_{eff} by transient measurement

The time derivative of (8) is

$$\dot{n} = \frac{\dot{V} b}{q W \mu_s(\Delta n)} \left[1 + \frac{\Delta n}{\mu_s(\Delta n)} \frac{d\mu_s}{d\Delta n} \right]^{-1} , \tag{9}$$

where the term in square brackets results from the dependence of $\mu_s(\Delta n)$ on Δn and therefore t. It is derived by making use of the relation, $d\mu_s/dt = d\mu_s/d\Delta n * d\Delta n/dt$, and is plotted in Figure B1(b). For $G = 0$, (7) and (9) combine to give

$$\tau_{eff} = -\frac{\Delta n}{\dot{n}} = -\frac{\Delta V}{\dot{V}} \left[1 + \frac{\Delta V b}{q W [\mu_s(\Delta n)]^2} \frac{d\mu_s}{d\Delta n} \right] , \tag{10}$$

which simplifies for constant $\mu_s(\Delta n)$ to

$$\tau_{eff} = -\frac{\Delta V}{\dot{V}} = \tau_{sig} \ , \tag{11}$$

where τ_{sig} is the exponential time constant of the excess photoconductance decay signal.

The important insight from this representation is that for a transient measurement, $\delta\tau_{eff}$ depends only on $\delta\tau_{sig}$ over the range of Δn where $\mu_s(\Delta n)$ is constant. Unfortunately, the calculation of $\delta\tau_{sig}$ is not elementary, requiring an assessment of an exponential fit to $\Delta V \pm \delta\Delta V$ against t. In this work, we determine $\delta\tau_{sig}$ from the 95% confidence interval associated with a least-squares error-weighted straight-line fit to a plot of $\ln(V)$ against t, where the errors in $\ln(V)$ arise from the resolution and noise of the voltage measurement, and the errors in t are negligible when using the 12-bit card of the WCT-100. Such fits can be performed with Origin [5].

Over the range where $\mu_s(\Delta n)$ is not constant, $\delta\tau_{eff}$ is even more difficult to calculate—as evident from (10)—being dependent on $\delta\Delta V$, δb, δW and $\delta\mu_s$ as well as $\delta\tau_{sig}$. Thankfully, the contributions from $\delta\Delta V$, δb, δW and $\delta\mu_s$ are usually small due to the factor of $d\mu_s/d\Delta n$.

3.3 Effective lifetime τ_{eff} by QSS measurement

When $\dot{n}$ is negligible, (7) and (8) combine to give,

$$\tau_{eff} = \frac{b}{q k \mu_s(\Delta n)} \frac{\Delta V}{V_{ref}} \ . \tag{12}$$

It is clear that $\delta\tau_{eff}$ associated with QSS measurements depends on the uncertainty of many more parameters than the transient case. Specifically, it depends δb, δk, $\delta\mu_s$, $\delta\Delta V$ and δV_{ref} for all Δn. Interestingly, it does not depend directly on δW due to the inclusion of W in the conversion of V_{ref} into G—see Equation (4)—although the uncertainty in W may contribute slightly to the choice of k, as discussed later.

We emphasise that QSS measurements contain a larger degree of uncertainty than transient measurements, and note that $\delta\Delta V$, δb, and $\delta\mu_s$ contribute to the error bars for both x and y axes in a plot of $\tau_{eff}(\Delta n)$.

3.4 Generalised analysis

When neither G nor $\dot{n}$ can be neglected, (4), (7), (8) and (9) combine to give

$$\tau_{eff} = \frac{\Delta V}{\frac{q k \mu_s(\Delta n)}{b} V_{ref} - \dot{V}} \ , \tag{13}$$

which, needless to say, leads to a complicated assessment of $\delta\tau_{eff}$ that depends on all input parameters.

4 UNCERTAINTY IN THE INPUT PARAMETERS

The uncertainty in Δn and τ_{eff} can be related to the uncertainty in the input parameters by applying the procedures of Appendix C to the equations of Section 3. The input uncertainties themselves depend on the instrumentation and experimental procedures and can

vary greatly from one PC experiment to another. They are now described for a reasonably careful measurement of c-Si wafers using the WCT-100 instrument. The resulting uncertainty in Δn and τ_{eff} are plotted for transient and QSS examples in the following section.

4.1 Uncertainty in PC calibration constants: δa, δb

The conventional way to determine the calibration constants is to measure V for wafers of known S (with no illumination). The symbols of Figure 1 show calibration data from the ANU using four non-diffused wafers (with nominal resistivities of 50, 8, 1 and 0.5 Ω-cm) and 11 wafers with uniform phosphorus diffusions. In the case of the non-diffused samples, S was calculated from the nominal resistivity and the width, while for the diffused samples, S was measured by four-point probe. In both cases, the associated uncertainty is depicted by error bars.

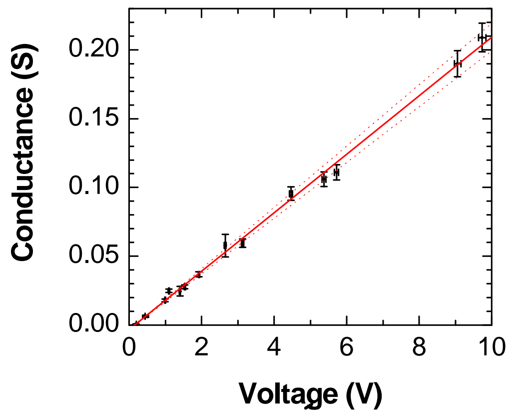

Figure 1: Symbols show calibration data, solid line shows a linear fit, and dotted lines show upper and lower limits to the 95% confidence interval.

The calibration constants and their associated uncertainty were then determined by a least-squares fit with an error-weighted 95% confidence interval (CI). Both linear and parabolic fits were achieved with Origin [5]. Table 1 lists the results, showing that the linear fit provides an accurate representation of the data, and when all wafers are included, b has a 95% CI of 3.3%. This value is used for $\delta b/b$ in the next section.

Note that the WCT-100 is commonly calibrated with just a few undiffused wafers. To demonstrate the subsequent uncertainty, Table 1 includes the calibration parameters associated with using only the four undiffused wafers; the 95% CI is 37%.

We further note that the calibration can drift over time introducing an additional source of uncertainty into δa and δb.. In the examples that follow, the measurements were conducted within days of the calibration and we have neglected any error due to drift.

Table 1: Calibration parameters and 95% CIs.

	a (S/V^2)		b (S/V)	
Using all calibration wafers				
Linear fit:			0.0213	±0.0007
Parabolic fit:	–0.0007	±0.0025	0.0216	±0.0004
Using four undiffused wafers				
Linear fit:			0.0215	±0.0079
Parabolic fit:	+0.001	±0.028	0.020	±0.053

Finally, the dark conductance of the experimental samples is sufficiently high to avoid the non-linear response of the WCT-100 at very low conductance [6].

4.2 Uncertainty in reference calibration constant δk

The uncertainty in k can be difficult to ascertain. It depends on the linearity of the reference detector to illumination (cell with resistor), on the reflection and width W of the sample, on the spectrum of the illumination, on the uncertainty in the detector against which that detector was calibrated, and on the difference in illumination on the detector and on the sample.

Fortunately, the uncertainty can also be assessed by applying the self-consistent calibration procedure of Trupke *et al.* [7], or by a comparison of QSS and transient analyses [8]. In this work, we estimate $\delta k/k$ at 3%.

4.3 Uncertainty in width of quasi-neutral base δW

The experimental samples were measured by a Mitutoyo digital micrometer (1DC-112E) with a nominal accuracy of ±3 μm. The samples and instrument were first cleaned to remove silicon particles (which cause gross overestimates of W), and then measured five times at five locations. The standard deviation of the mean was ±1 μm. Thus, we conclude the wafer width is measured to ±4 μm. To convert the wafer width to the width of the quasi-neutral base, we subtracted 2 ± 1 μm to account for the diffusion and depletion widths, and therefore use δW = ±5 μm.

4.4 Uncertainty in output voltages: δV and δV_{ref}

The WCT-100 measures $V(t)$ and $V_{ref}(t)$ at 12-bit resolution for both voltage and time with a sample rate of 5 MHz. Such resolution leads to negligible uncertainty when compared to the noise, provided the most suitable gain and dynamic range is utilised. The best resolution would be attained from the highest gain (±0.2 V), where 12 bits provides ±100 μV, which corresponds to a resolution in Δn of $\pm 2.4 \times 10^{11}$ cm^{-3} for a 300 μm thick wafer using the above calibration.

Although shielded, the detectors and associated electronics pick up ambient noise and introduce noise themselves. The WCT-100 reduces this noise by averaging the sampled data to 125 data points; thus for a 12 ms signal (as used in conventional QSS experiments), each data point is a 480-point average, reducing the random noise by a factor of ~22 ($\sqrt{480}$). (Note that when the illumination source decays exponentially, V and V_{ref} also decay exponentially and the multi-point average tends to overestimate V and V_{ref}. This uncertainty is small and omitted in the following examples, though it could be mitigated by applying a moving exponential fit rather than a multi-point average.)

The random noise can be further reduced by averaging multiple signals. In this work, we take $V(t)$ and $V_{ref}(t)$ to be the mean of 20 signals, and $\delta V(t)$ and $\delta V_{ref}(t)$ to be the standard deviation from the mean of those signals.

To determine $\Delta V(t) = V(t) - V_0$, the equilibrium voltage V_0 was determined as the average of 500,000 measurements over 100 ms. The associated random error δV_0 was negligible compared to $\delta V(t)$ and is neglected, and any systematic offset error in $V(t)$ and V_0 cancel in

the calculation of $\Delta V(t)$. Thus, $\delta\Delta V(t)$ was assumed equal to the random error $\delta V(t)$. Finally, $\delta\tau_{sig}$ was determined from $V(t) \pm \delta V(t)$ in the manner described in Section 3.2.

4.5 Uncertainty in the sum of carrier mobilities $\delta\mu_s$

In this work, $\mu_s(\Delta n)$ is calculated with Equation B1, which is a parameterised fit to existing experimental data for uncompensated monocrystalline silicon [9]. From the same data, we estimate $\delta\mu_s$ over any likely variation of T from 25 °C to be 10% of μ_s for all Δn. (The temperature-controlled WCT-100 stage is estimated to remain within δT < 2 °C of the calibration temperature.) Note that a larger $\delta\mu_s$ is appropriate for semiconductor materials that are less characterised than uncompensated monocrystalline silicon, such as compensated c-Si or µc-Si

A more thorough examination of $\delta\mu_s$ is desirable, but being systematic, this large uncertainty can be neglected from relative comparisons between PC experiments that use similar semiconductor materials and apply the same mobility model. .

4.6 Uncertainty in base doping concentration δN

Although not expressed directly within the equations of Section 3, the base doping concentration N is an input to (B1), which relates μ_s to Δn. In the examples that follow, δN was ascertained from the nominal resistivity range guaranteed by the wafer supplier, where the resistivity was converted into N using [10]. The uncertainty in the resistivity—and therefore N—can also be measured by four-point probe measurements or with the calibrated inductive coil itself. Alternatively, N and δN can be ascertained by SIMS. Table 2 lists N and δN for the examples of the following section.

Table 2: Doping concentration of experimental samples.

	N (cm^{-3})	δN (cm^{-3})
Wafer 1 (Transient):	4.6×10^{13}	0.8×10^{13}
Wafer 2 (QSS):	3.3×10^{15}	1.7×10^{15}

5 EXAMPLES

Two examples are provided: (1) a transient measurement on high-lifetime, phosphorus-diffused, oxidised, 444 µm float-zone silicon; and (2) a steady-state measurement on low-lifetime, phosphorus-diffused, 205 µm multi-crystalline silicon. Figures 2 and 3 presents the resultant $\tau_{eff}(\Delta n)$ where the error bars represent the uncertainty. The data in both figures is the composite of several measurements of different gain; in this way, many orders of magnitude can be studied with high resolution.

Figures 2 and 3 plot the results when the systematic error, $\delta\mu_s$, is (a) included and (b) omitted. Their comparison reveals that for the transient measurement, $\delta\mu_s$ affects $\delta\Delta n$ at high Δn but less so at low Δn where $\delta\Delta V$ is the largest source of uncertainty; $\delta\mu_s$ has negligible influence on $\delta\tau_{eff}$ which is dominated by $\delta\tau_{sig}$. For QSS measurements, $\delta\mu_s$ affects both $\delta\Delta n$ and $\delta\tau_{eff}$ at all Δn and is the dominant source of absolute uncertainty; when omitted, the dominant sources of uncertainty are δb and δk, the latter of which affects just $\delta\tau_{eff}$ (see Section 3).

Table 3 lists τ_{eff} and $\delta\tau_{eff}$ at $\Delta n = 10^{15}$ cm^{-3}. In the transient example, the steep slope of $\tau_{eff}(\Delta n)$ at Δn =

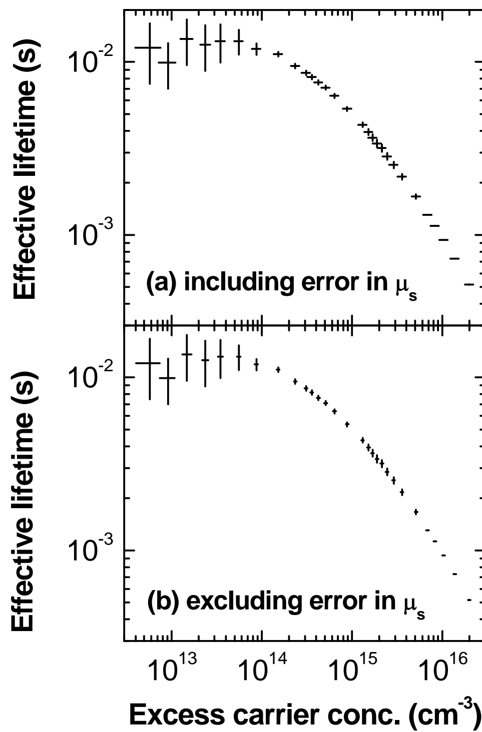

Figure 2: $\tau_{eff}(\Delta n)$ for Example 1 (transient). For clarity, the data plots just every tenth data point.

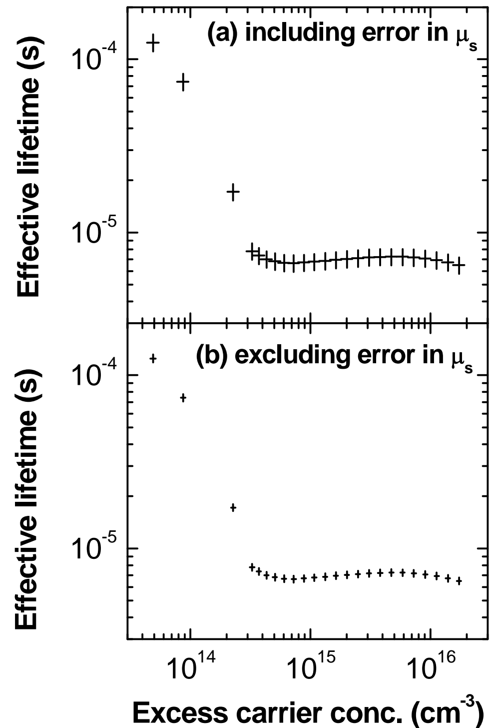

Figure 3: $\tau_{eff}(\Delta n)$ for Example 1 (transient). For clarity, the data plots just every fifth data point.

Table 3: τ_{eff} and $\delta\tau_{eff}$ at $\Delta n = 10^{15}$ cm^{-3}.

	τ_{eff} (µs)	$\delta\tau_{eff}$ (µs)	$\delta\tau_{eff}/\tau_{eff}$
Including $\delta\mu_s$			
Example 1 (transient):	5010	430	8.6%
Example 2 (QSS):	6.77	0.74	10.9%
Excluding $\delta\mu_s$			
Example 1 (transient):	5010	150	3.0%
Example 2 (QSS):	6.77	0.30	4.5%

10^{15} cm^{-3} increases $\delta\tau_{eff}$ due to the error in Δn. Regardless, the transient example is found with significantly more certainty than the QSS measurement, particularly when $\delta\mu_s$ is omitted (due to its affect on Δn).

Finally, we note that the sudden increase in τ_{eff} below $\Delta n = 5 \times 10^{14}$ cm^{-3} in Figure 3 is due to trapping in the multi-crystalline silicon. This measurement artefact arises due to the invalidity of Assumption (c) in Appendix A.

6 DISCUSSION

The above experiments were taken reasonably carefully, and as such, the uncertainty in the results is relatively small. Nevertheless, they might be improved by (in order of importance): a detailed study of $\delta\mu_s$, a more accurate calibration of the reference detector, more averaging of the voltage signals, and a SIMS measurement to determine $N \pm \delta N$.

Many PC studies contain a higher degree of uncertainty than that presented here. Typically, this is introduced by one or more of the following factors.

(1) Differing illumination over the wafer and the reference detector. This occurs particularly when the lamp is placed close to the sample to obtain high carrier densities or to measure low-lifetime samples. The associated δk can be large, affecting QSS measurements.

(2) The use of few samples to calibrate the PC coil, introducing a large δa and δb (see Section 4.1).

(3) The measurement of samples within containers (transparent bags or petri dishes) when the coil was calibrated on bare wafers; or equivalently, the measurement of thick samples when the coil was calibrated with thin wafers, or vice versa. Both procedures raise δa and δb due to the distance-dependence of the coil's sensitivity.

(4) The use of suboptimal gains in the measurement of $V_{ref}(t)$ and $V_{ref}(t)$, leading to high δV, δV_{ref} and $\delta\tau_{sig}$.

(5) Heating of the wafer during measurement, which varies μ_s over the course of the illumination pulse. This can be observed in heavily-doped wafers where ΔS due to varying μ_s can be comparable to ΔS due to varying Δn. (This is most important when one neglects $\delta\mu_s$ as a systematic error.)

(6) Experiments in which the assumptions in Appendix A are invalid, such as those on wafers with trapping [11] or depletion-region modulation [12], those with spatially varying recombination or photogeneration (the latter being most significant when the lamp is placed close to large wafers); and those at a sufficiently high Δn that Δn varies considerably across the wafer thickness.

7 CONCLUSION

A preliminary study into the uncertainties associated with PC measurements was presented. The associated equations were written in terms of input parameters, from which it is evident that transient measurements are influenced by many fewer uncertainties than QSS measurements. Quantification of the resultant uncertainty in τ_{eff} and Δn is not trivial due to the implicit relationship between μ_s and Δn, to the quantification of calibration errors, and in the transient case, to the quantification of the error in the voltage decay constant. Nevertheless, the uncertainty can still be calculated and two examples were provided: one high-lifetime transient measurement and one low-lifetime QSS measurement. The examples plotted $\tau_{eff}(\Delta n)$ with and without the systematic error in μ_s, where the latter is sufficient to compare relative measurements that apply the same mobility model. A more detailed assessment of PC uncertainties is in preparation, one that will also include the uncertainty in emitter saturation current and bulk lifetime.

8 REFERENCES

[1] www.sintonconsulting.com.

[2] H. Nagel *et al.*, *J. Appl. Phys.* **86**: 6218–6221 (1999).

[3] D.E. Kane and R.M. Swanson, *IEEE PVSC* (1985), 578–893.

[4] R.A. Sinton and A. Cuevas, *Appl. Phys. Lett.* **69**: 2510–2512 (1996).

[5] Origin 6.1, OriginLab Corporation, Northampton, USA.

[6] K.R. McIntosh *et al.*, *Progress in Photovoltaics*, **16**: 279–287 (2008).

[7] T. Trupke *et al.*, *Appl. Phys. Lett.* **87**:184102-1-3 (2005).

[8] D. Macdonald *et al.*, *20th EC PVSEC*, Barcelona,. (2005), 627–630.

[9] P.P. Altermatt *et al.*, *16th EU PVSEC*, Glasgow (2000), 243–246.

[10] W.R. Thurber *et al.*, *J. Electrochem. Soc.* **127**: 1807–1812 (1980); W.R. Thurber *et al.*, *J. Electrochem. Soc.* **127**: 2291–2294 (1980).

[11] D. Macdonald and A. Cuevas, *Appl. Phys. Lett.* **74**: 1710–1712 (1999).

[12] P.J. Cousins *et al.*, *J. Appl. Phys.* **95**: 1854–1858 (2004); M. Bail *et al.*, *Appl. Phys. Lett.* **82**: 757–759 (2003).

[13] S. Reggiani *et al.*, *IEEE Trans. Electron Devices* **49**: 490–499 (2002); N.D. Arora *et al.*, *IEEE Trans. Electron Devices* **29**: 292 (1982); J.M. Dorkel and P. Leturcq, *Solid-State Electronics* **24**: 821–825 (1981).

[14] J.R. Taylor, *An Introduction to Error Analysis*, 2nd ed., University Science Books (1997), p. 75.

APPENDIX A: GENERAL ASSUMPTIONS

The scope of the analysis is limited by the following assumptions, all of which are invoked in most PC studies.

(a) Carrier flow is one dimensional (perpendicular to the plane of the wafer), requiring diffusion profiles, wafer width, bulk resistivity, and carrier generation to be spatially uniform, and requiring there be no shunting or edge recombination.
(b) Carrier concentrations are constant in the bulk of the wafer, requiring the sample to be vertically symmetric (i.e., identical diffusions and/or passivation on front and rear) and recombination at the surfaces and in the diffusions to be small.
(c) Excess carrier concentrations of electrons Δn and holes Δp are equal, requiring the sample to be charge-neutral and to contain no significant trapping (i.e. no illumination-dependent defect occupation) [11].
(d) Depletion-region modulation is negligible, making the effective width of the base constant for all illumination [12].
(e) Excess conductance in any surface diffusion is negligible compared to that in the quasi-neutral base.
(f) Temperature and calibration constants are time-independent.

When (c) and (d) are valid, PC analyses are simplified by requiring just the mobility sum: $\mu_s = \mu_n + \mu_p$.

APPENDIX B: CARRIER MOBILITY IN C-SI

The parameter that most complicates error analyses of PC experiments on uncompensated monocrystalline c-Si wafers is μ_s. It depends on carrier and doping concentration as well as temperature [13]. While an assessment of these dependencies is beyond the scope of this paper, we note that the parameterisation of μ_s in the WCT-100 software has proven reasonable at 25 °C [9]; it depends on N and Δn but not on the dopant species or temperature:

$$\mu_s = 1800\left[\frac{1+f(\Delta n+N)}{1+8.36f(\Delta n+N)}\right], \tag{B1}$$

where N is the doping density and

$$f(\Delta n+N) = \left(\frac{\Delta n+N}{1.2\times10^{18}}\right)^{0.8431}. \tag{B2}$$

Figure B1(a) plots (B1) for various N. It shows that $\mu_s = 1800$ cm^{2}V^{-1}s^{-1} when $\Delta n + N$ is small (i.e., intrinsic silicon), and that μ_s is constant in low injection ($\Delta n \ll N$).

This dependence of μ_s on Δn introduces an implicit equation into PC analyses—a relationship that greatly complicates the calculation of PC uncertainties.

Note that an alternative parameterisation to (B1) may be required to describe $\mu_s(\Delta n)$ for other silicon materials, such as compensated c-Si or µc-Si.

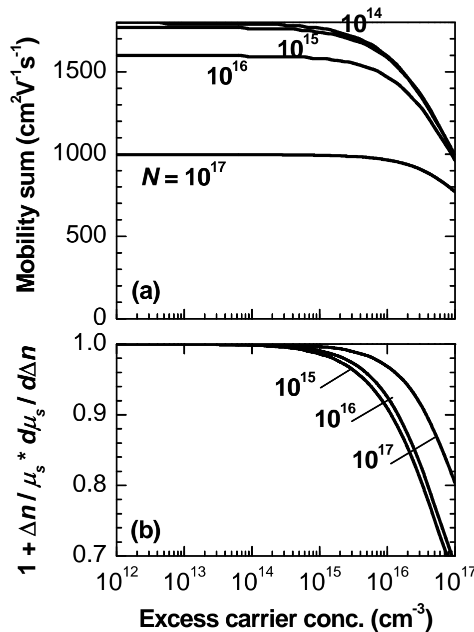

Figure B1: **(a)** μ_s and **(b)** $\left[1-\Delta n/\mu_s \cdot d\mu_s/d\Delta n\right]^{-1}$ as a function of Δn from (B1) for a range of N.

APPENDIX C: UNCERTAINTY

Method I: Application of upper & lower limits

The upper and lower limits of a parameter, $q(x, ..., z)$, can be calculated from the appropriate upper and lower limits of its constituents. For example, when $q(x, y) = x/y$, q's upper limit is $q + \delta q = (x + \delta x)/(y - \delta y)$, and its lower limit is $q - \delta q = (x - \delta x)/(y + \delta y)$. In this case, the upper limit to q requires the upper limit to x and the lower limit to y; the converse applies for q's lower limit.

This method to calculate the uncertainty in $q(x, ..., z)$ is conceptually simple and applicable to the implicit equations that arise in PC analysis. The method can, however, be unnecessarily conservative.

Method II: Analytical equations

The uncertainty of parameter, $q(x, ..., z)$, lies within the limits [14],

$$\sqrt{\left(\left|\frac{\partial q}{\partial x}\right|\delta x\right)^2 + \ldots + \left(\left|\frac{\partial q}{\partial z}\right|\delta z\right)^2} \le \delta q \le \left|\frac{\partial q}{\partial x}\right|\delta x + \ldots + \left|\frac{\partial q}{\partial z}\right|\delta z ,$$

where the lower limit arises when the uncertainty of the input parameters is independent and random, and the upper limit is essentially the same as that found by Method I. Thus, at either extreme, an equation can be used to determine δq when $q(x, ..., z)$ is explicit.

In this work, we apply the lower limit of Method II when the input variables are clearly random and independent and the associated equation is analytic, and Method I otherwise.